Journal of Alloys and Compounds 480 (2009) 765–770

Journal of Alloys and Compounds

journal homepage: www.elsevier.com/locate/jallcom

Corrosion resistance of electrodeposited Ni–B and Ni–B–Si_3N_4 composite coatings

K. Krishnaveni [a], T.S.N. Sankara Narayanan [a,*], S.K. Seshadri [b]

[a] National Metallurgical Laboratory, Madras Centre CSIR Complex, Taramani, Chennai 600 113, India
[b] Department of Metallurgical and Materials Engineering, Indian Institute of Technology, Chennai 600 036, India

ARTICLE INFO

Article history:
Received 4 June 2008
Received in revised form 1 February 2009
Accepted 13 February 2009
Available online 27 February 2009

Keywords:
Nanostructures
Surfaces and interfaces
Nanofabrications
X-ray diffraction
Electrochemical reactions

ABSTRACT

Corrosion resistance of electrodeposited (ED) and electroless (EL) composite coatings have been a debatable issue in the published literature. The present paper aims to compare the corrosion resistance of ED Ni–B–Si_3N_4 composite coating with its plain counter part. The ED Ni–B coatings were prepared using Watt's nickel bath modified with the addition of dimethylamine borane and the ED Ni–B–Si_3N_4 composite coatings were prepared using the same bath in which Si_3N_4 particles (mean diameter: 0.80 μm) were dispersed in it. The structural and morphological characteristics of ED Ni–B and Ni–B–Si_3N_4 composite coatings were determined using X-ray diffraction (XRD) measurements and scanning electron microscopy (SEM). The corrosion resistances of ED Ni–B and Ni–B–Si_3N_4 composite coatings, both in as-plated and heat treated conditions, in 3.5% NaCl, were evaluated by potentiodynamic polarization and electrochemical impedance spectroscopy (EIS) studies. The study reveals that the extent of shift in corrosion potential (E_{corr}) towards the noble direction, decrease in corrosion current density (i_{corr}), increase in charge transfer resistance (R_{ct}) and decrease in double layer capacitance (C_{dl}) values with the incorporation of Si_3N_4 particles in the ED Ni–B matrix is not appreciable, both in as-plated and heat-treated conditions. The occurrence of the second phase angle maximum suggests penetration of the electrolyte via the pores/micro-pores in these coating to create another interface, namely, the electrolyte/substrate. Unlike the nanosized particles, the micron size Si_3N_4 particles (mean diameter: 0.80 μm) used in this study is not capable of completely filling all the pores in the coating and allowed diffusion of chloride ions along the interface. The marginal improvement in corrosion resistance observed for ED Ni–B–Si_3N_4 composite coatings compared to its plain counterpart could have resulted from the decrease in effective metallic area prone to corrosion.

1. Introduction

The idea of codepositing various second phase particles in electrodeposited (ED) and electroless (EL) metal matrix and thereby taking advantage of their desirable qualities, such as high hardness, excellent wear and abrasion resistance, improved corrosion resistance, etc. has led to the development of composite coatings with a wide range of possible combination and properties [1–6]. A number of oxides, carbides and nitrides were used as second phase particles to produce ED or EL composite coatings. Silicon nitride (Si_3N_4) is a very hard ceramic material, which retains its room temperature strength up to 1200 °C and possesses excellent dimensional stability and oxidation resistance. The Si_3N_4 particles were successfully codeposited in ED Ni, ED Ni–P, ED Ni–Co and EL Ni–P matrix by dispersing them in the respective plating baths [6–14]. Codeposition of Si_3N_4 particles in ED Ni matrix has also been shown possible by brush plating technique [15]. The incorporation of Si_3N_4 particles in ED or EL Ni or Ni alloy matrix enables an increase in the hardness and improvement in the tribological behaviour [6–14]. The use of ED and EL Ni–P–Si_3N_4 composite coating has been explored for a variety of industrial components [8,11]. Wang et al. [8] have reported that ED Ni–P–Si_3N_4 composite coated aluminium piston skirt offers moderate scuffing and wear resistance when subjected to rubbing against an aluminum cylinder bore. Das et al. [11] have reported that EL Ni–P–Si_3N_4 composite coated SAE 52100 bearing steel offers significant improvement in wear resistance under water lubricated conditions and recommend their use for ferrous based bearings for water lubricated applications. However, it is important to note that the type of metal matrix in which the second phase particles are incorporated also plays a vital role in achieving the desired performance. Xinmin and Zonggang [16] have suggested that the metal matrix should be capable of supporting the second phase particle to achieve better wear resistance, both in as plated

* Corresponding author. Tel.: +91 44 2254 2077; fax: +91 44 2254 1027.
E-mail addresses: tsnsn@rediffmail.com, tsnsn2005@yahoo.co.in (T.S.N.S. Narayanan).

0925-8388/$ – see front matter © 2009 Elsevier B.V. All rights reserved.
doi:10.1016/j.jallcom.2009.02.053

Table 1
Bath composition and operating conditions used to prepare ED Ni–B–Si_3N_4 composite coatings.

Bath composition	
Nickel sulphate hexahydrate	240 g/l
Nickel chloride hexahydrate	45 g/l
Boric acid	30 g/l
Dimethylamine borane	3 g/l
Si_3N_4 powder	50 g/l
Operating conditions	
Temperature	45 ± 1 °C
pH	3.5
Current density	1 A/dm^2
Agitation	Mechanical – using magnetic stirrer at 600 rpm
Time	120 min

and heat-treated conditions. Both ED and EL Ni–B alloy matrix possess high hardness and superior wear resistance [17–19]. Hence, they can be considered as an ideal choice for the incorporation of second phase particles. Studies on ED and EL Ni–B based composite coatings are rather limited. The formation and characteristics of ED Ni–B–Si_3N_4 composite coating was reported in our earlier paper [20]. Corrosion resistance of ED and EL composite coatings has been a debatable issue in the published literature. The present paper aims to compare the corrosion resistance of ED Ni–B and Ni–B–Si_3N_4 composite coatings.

2. Experimental

Mild steel discs (30 mm diameter and 5 mm thick, having a composition of C: 0.16%; Si: 0.18%; Mn: 0.62%; P: 0.012%; S: 0.016%; Cr: 0.01%; Ni: 0.1%; Fe: balance) were used as the substrate material for the electrodeposition of Ni–B and Ni–B–Si_3N_4 composite coatings. The particle size of the Si_3N_4 particles was determined by Cilas particle size analyzer. The Si_3N_4 particles have a d_{10}, d_{50} and d_{80} of 0.08, 0.39 and 0.92 μm, respectively, with a mean diameter of 0.80 μm. The d_{10}, d_{50} and d_{80} are the average diameter of 10%, 50% and 80% of the Si_3N_4 particles. The details of surface preparation, electrodeposition cell, chemical analysis of nickel, boron and the level of incorporation of Si_3N_4 particles, were already presented in our earlier papers [17,20]. The chemical composition of the plating bath and its operating conditions are given in Table 1. The structure of ED Ni–B and Ni–B–Si_3N_4 composite coatings, both in as-plated and heat treated (400 °C for 1 h) conditions, was determined by X-ray diffraction (XRD) measurements using Cu K_α (λ = 1.5418 Å) radiation. The surface morphology of these coating was assessed by scanning electron microscopy (SEM). The surface roughness of ED Ni–B–Si_3N_4 composite coating was determined from the surface profile obtained using a Carl Zeiss laser scanning microscope (Model, LSM5 PASCAL).

The corrosion resistance of ED Ni–B and Ni–B–Si_3N_4 composite coatings, both in as-plated and heat treated (400 °C for 1 h) conditions, in 3.5% NaCl, was evaluated by potentiodynamic polarization and electrochemical impedance spectroscopy (EIS) studies using a potentiostat/galvanostat/frequency response analyzer (ACM Instruments, UK; Model: Gill AC). The thickness of these coatings used for evaluating the corrosion resistance was 20 ± 1 μm. The ED Ni–B and Ni–B–Si_3N_4 composite coated mild steel were used as the working electrode while a saturated calomel electrode and a graphite rod served as the reference and counter electrodes, respectively. These electrodes were placed in a flat cell in such a way that only 1 cm^2 area of the working electrode was exposed to the electrolyte solution. The corrosion potential (E_{corr}) and corrosion current density (i_{corr}) were determined from the polarization curves using Tafel extrapolation method. Both Nyquist and Bode plots were used to understand the corrosion behaviour of ED Ni–B and Ni–B–Si_3N_4 composite coated mild steel. The impedance values of the coatings were calculated from Bode impedance plots. The Bode phase angle plots were also analyzed to understand the mechanism of corrosion of ED Ni–B and Ni–B–Si_3N_4 composite coated mild steel.

3. Results and discussion

3.1. Characteristics of ED Ni–B and Ni–B–Si_3N_4 composite coatings

The plating rate of ED Ni–B and Ni–B–Si_3N_4 composite coatings is about 12 μm/h. The incorporation of Si_3N_4 particles in the ED Ni–B matrix decreases the metallic lustre, increases the surface roughness and alters the chemical composition. Similar phenomena were also observed earlier by Muller et al. [21] and Novakovic et al. [22]. The average surface roughness (R_a) of ED Ni–B–Si_3N_4 composite coatings is 1.17 μm. The chemical composition of coating changes from 97 wt.% Ni and 3 wt.% B to 89.6 wt.% Ni; 2.4 wt.% B and 8 wt.% Si_3N_4 with the incorporation of Si_3N_4 particles in the ED Ni–B matrix. The surface morphology of ED Ni–B and Ni–B–Si_3N_4 composite coatings is shown in Fig. 1(a and b), respectively. ED Ni–B coatings reveal the formation of well-crystallized, uniform and fine-grained deposits, with some cracks that might have emerged due to the stress in the coating (Fig. 1(a)). The ED Ni–B–Si_3N_4 composite coatings consist of a homogeneous fine globular structure in which the Si_3N_4 particles are uniformly distributed on the surface of the matrix (Fig. 1(b)). The X-ray diffraction patterns of as-plated ED Ni–B and Ni–B–Si_3N_4 composite coatings are shown in Fig. 2(a) and 2(b), respectively. The XRD pattern of as-plated ED Ni–B coating indicates that the nucleation of the nickel phase in not completely prevented since the extent of alloying of boron is relatively low. However, alloying of boron with nickel causes a change in the preferred orientation of the Ni–B coating with Ni (1 1 1) being the most intense reflection. It is evident from Fig. 2(b) that the incorporation of Si_3N_4 particles causes a significant change in structure of the ED Ni–B–Si_3N_4 composite coatings. The absence of the reflection from Ni (2 0 0) plane and the change in intensity and broadening of the reflection from Ni (1 1 1) plane suggest a change in crystal orientation of the coating following incorporation of the Si_3N_4 particles in the ED Ni–B matrix. The change in crystal orientation following the incorporation of second phase particles in ED and EL compos-

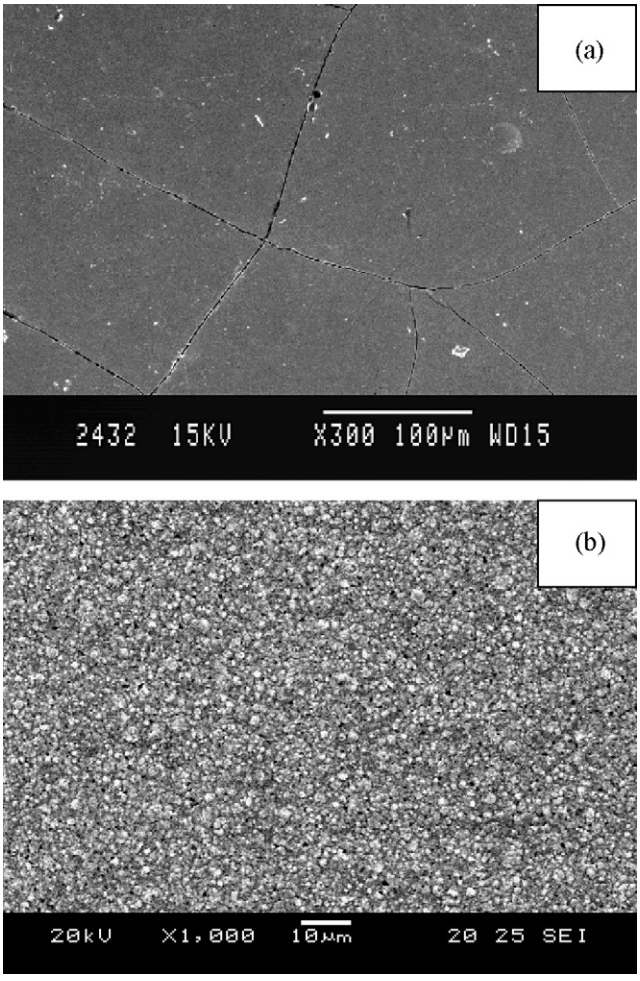

Fig. 1. Scanning electron micrographs of ED Ni–B and Ni–B–Si_3N_4 composite coatings: (a) ED Ni–B and (b) ED Ni–B-Si_3N_4.

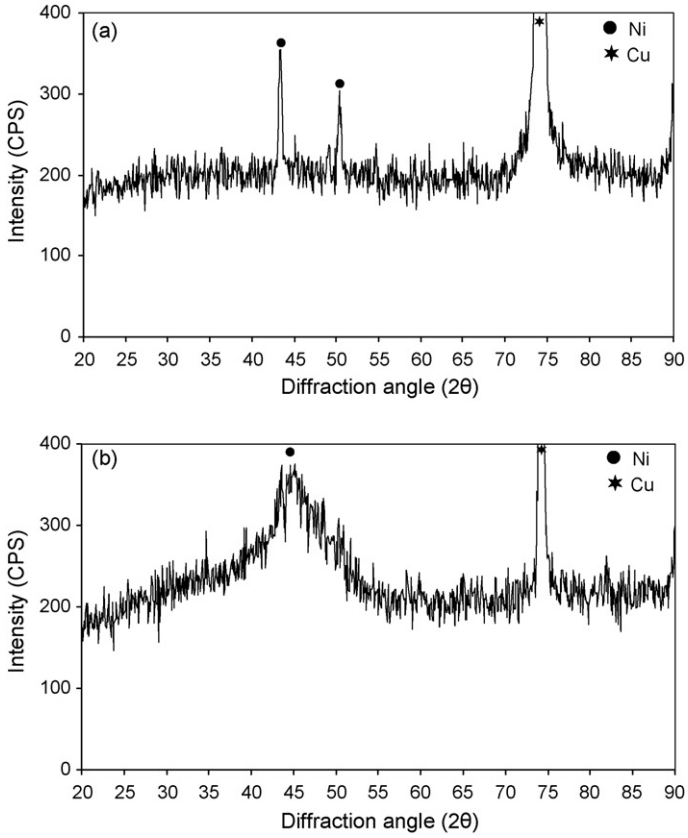

Fig. 2. X-ray diffraction patterns of as-plated ED Ni–B and Ni–B–Si_3N_4 composite coatings: (a) ED Ni–B; and (b) ED Ni–B–Si_3N_4.

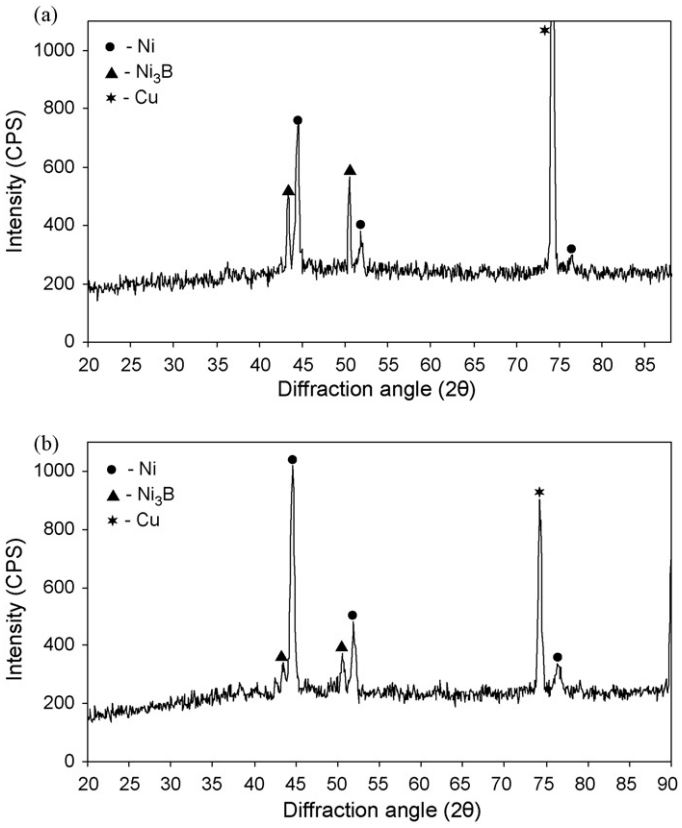

Fig. 3. X-ray diffraction patterns of ED Ni–B and Ni–B–Si_3N_4 composite coatings after heat-treatment at 400 °C for 1 h: (a) ED Ni–B; and (b) ED Ni–B–Si_3N_4.

ite coatings has been reported earlier by many researchers [23–26]. The grain size of as-plated ED Ni–B and Ni–B–Si_3N_4 composite coating is 10–13 and 6–8 nm, respectively. The XRD patterns of ED Ni–B and Ni–B–Si_3N_4 composite coatings after heat-treatment at 400 °C for 1 h are shown in Fig. 3(a) and 3(b), respectively. It is evident from Fig. 3 that heat-treatment increases the crystallinity of these coatings and enables the formation of Ni_3B phase. The Ni (1 1 1) texture is retained even after heat-treatment. The intensity of the reflection from Ni (1 1 1) plane of ED Ni–B–Si_3N_4 composite coating is relatively higher than that of ED Ni–B coating, which further confirms the change in crystal orientation following the incorporation of Si_3N_4 particles in the ED Ni–B matrix. Heat-treatment increases the grain size of both ED Ni–B and Ni–B–Si_3N_4 composite coatings. After heat-treatment at 400 °C for 1 h, the grain size of ED Ni–B and Ni–B–Si_3N_4 composite coatings are increased to 17–20 and 12–14 nm, respectively.

3.2. Corrosion resistance of ED Ni–B and Ni–B–Si_3N_4 composite coating

The potentiodynamic polarization curves of ED Ni–B and Ni–B–Si_3N_4 composite coatings in 3.5% NaCl, both in as-plated and heat-treated (400 °C for 1 h) conditions are shown in Fig. 4. The corrosion potential (E_{corr}) and corrosion current density (i_{corr}), calculated using the Tafel extrapolation method, are given in Table 2. The E_{corr} of ED Ni–B and Ni–B–Si_3N_4 composite coatings, in their as-plated conditions are −584 and −560 mV vs. SCE, respectively, and the corresponding i_{corr} values are 12.31 and 10.92 μA/cm^2. Heat-treatment of ED Ni–B and Ni–B–Si_3N_4 composite coating at 400 °C for 1 h results in a cathodic shift in the E_{corr} (from −584 to −680 mV vs. SCE for ED Ni–B coating and from −560 to −665 mV vs. SCE for ED Ni–B–Si_3N_4 composite coating) and an increase in i_{corr} (from 12.31 to 24.30 μA/cm^2 for ED Ni–B coatings and from 10.92 to 21.98 μA/cm^2 for ED Ni–B–Si_3N_4 composite coating).

The Nyquist plots of ED Ni–B and Ni–B–Si_3N_4 composite coatings in 3.5% NaCl, both in as-plated and heat-treated (400 °C for 1 h) conditions, at their respective open circuit potentials, are shown in Fig. 5. It is evident from Fig. 5 that ED Ni–B and Ni–B–Si_3N_4 composite coatings, both in as-plated and heat-treated conditions (400 °C for 1 h), exhibit a semicircle in the high frequency region followed by a loop in the low frequency region. Though the curves in the Nyquist plot appear to be similar with respect to their shape, they differ considerably in their size. This indicates that same fundamental processes must be occurring on both the as-plated and heat-treated Ni–B and Ni–B–Si_3N_4 composite coatings but over a different effective area in each case. The formation of a single semi-

Table 2
Corrosion resistance of ED Ni–B and ED Ni–B–Si_3N_4 composite coatings in their as-plated and heat-treated conditions in 3.5% NaCl evaluated by potentiodynamic polarization and electrochemical impedance (EIS) studies.

Type of coating	E_{corr} (mV vs. SCE)	i_{corr} (μA/cm^2)	R_{ct} (Ω cm^2)	C_{dl} (μF/cm^2)
ED Ni–B coating as-plated	−584	12.31	2100	116
ED Ni–B coating heat-treated (400 °C/1 h)	−680	24.10	1370	160
ED Ni–B–Si_3N_4 composite coating as-plated	−560	10.92	2020	98
ED Ni–B–Si_3N_4 composite coating heat-treated (400 °C/1 h)	−665	21.98	1400	148

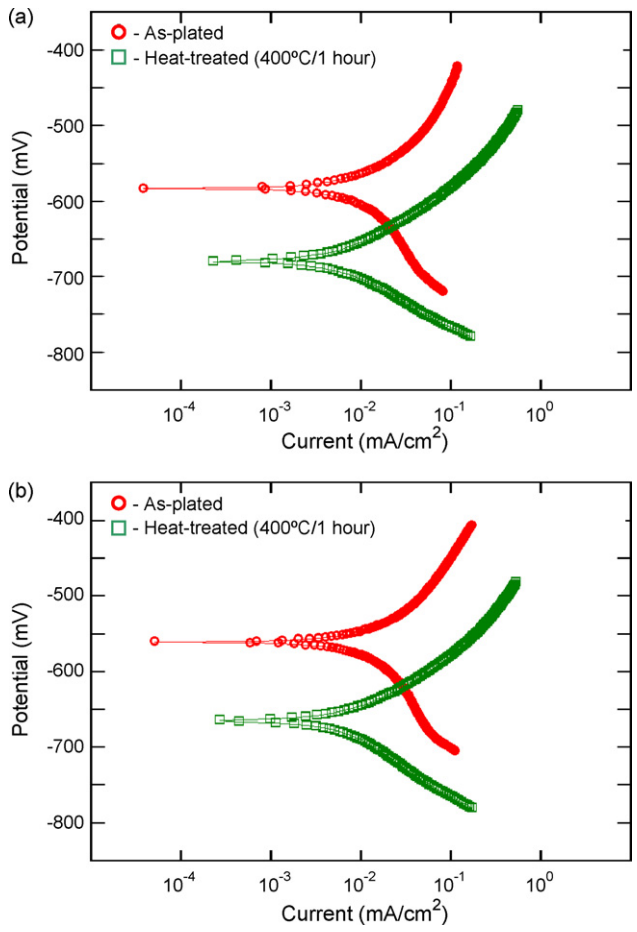

Fig. 4. Polarization curves of ED Ni–B and Ni–B–Si_3N_4 composite coatings in 3.5% NaCl in their as-plated and heat-treated (400 °C for 1 h) conditions (potential in mV vs. SCE): (a) ED Ni–B; and (b) Ni–B–Si_3N_4.

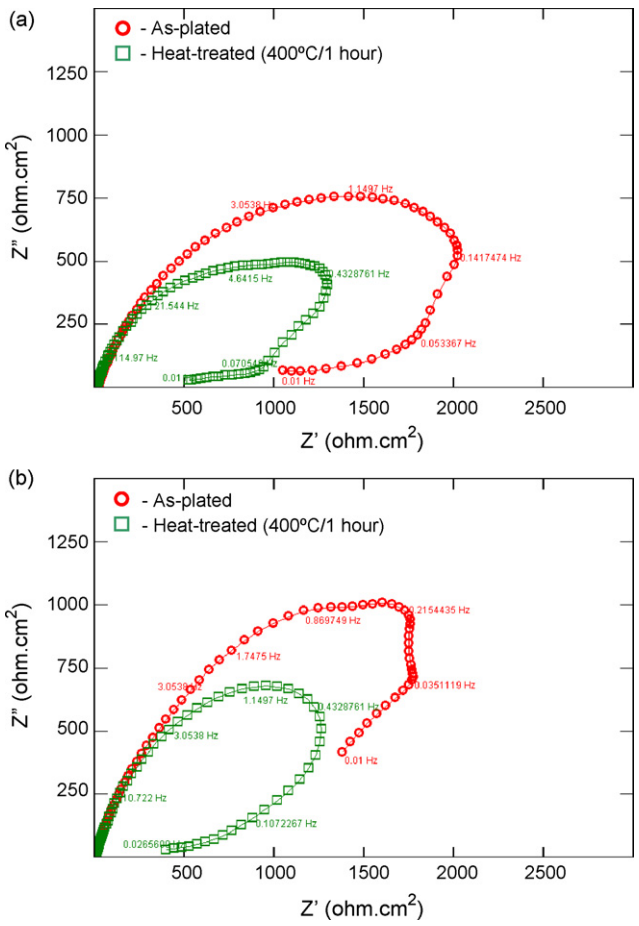

Fig. 5. Nyquist plots of ED Ni–B and Ni–B–Si_3N_4 composite coatings in 3.5% NaCl in their as-plated and heat-treated (400 °C for 1 h) at their respective open circuit potentials: (a) ED Ni–B; and (b) ED Ni–B–Si_3N_4.

circle or a semicircle in the high frequency region followed by a low frequency loop is typical of metallic coatings. The semicircle at high frequency region represents the coating response, while the loop at low frequency region is associated with simultaneous physico-chemical phenomena at the metal/coating/solution interface [27]. According to Mansfeld et al. [28] the loop at the lower frequency region is associated with the double layer capacitance and/or diffusion phenomena of the oxidant chemical species through the porous coating.

In order to get a better insight about the coating response as well as the diffusion phenomenon, Bode impedance ($\log f$ vs. impedance) and phase angle plots ($\log f$ vs. phase angle) were constructed. The Bode impedance plots of ED Ni–B and Ni–B–Si_3N_4 composite coating, both in as-plated and heat-treated conditions (400 °C for 1 h) (Fig. 6), indicate that these coatings offer a relatively better corrosion resistance in their as-plated condition and heat-treatment leads to a decrease in their corrosion protective ability. The Bode phase angle plots of ED Ni–B and Ni–B–Si_3N_4 composite coating, both in as-plated and heat-treated conditions (400 °C for 1 h), indicate the presence of two phase angle maxima (Fig. 7), suggesting the involvement of two time constants. The occurrence of these two phase angle maxima could be related to the electrolyte/coating and the electrolyte/substrate interface, respectively. The second phase angle maximum is related to the penetration of the electrolyte via the pores/micro-pores in the coating to create another interface, namely, the electrolyte/substrate. The occurrence of the second phase angle maximum is distinct for as-plated and heat-treated ED Ni–B coating. The Bode plots (Fig. 7) also indicate the involvement of a diffusion phenomenon in the low frequency region.

The R_{ct} and C_{dl} values of ED Ni–B and Ni–B–Si_3N_4 composite coatings, in their as-plated and heat-treated conditions (400 °C for 1 h) are compiled in Table 2. The R_{ct} of ED Ni–B and Ni–B–Si_3N_4 composite coatings, in their as-plated conditions are 2100 and 2020 Ohm.cm^2, respectively, and the corresponding C_{dl} values are 116 and 98 μF/cm^2. Heat-treatment of ED Ni–B and Ni–B–Si_3N_4 composite coating at 400 °C for 1 h results in a decrease in R_{ct} (from 2100 to 1370 Ω cm^2 for ED Ni–B coating and from 2020 to 1400 Ω cm^2 for ED Ni–B–Si_3N_4 composite coating) and an increase in C_{dl} (from 116 to 160 μF/cm^2 for ED Ni–B coatings and from 98 to 148 μF/cm^2 for ED Ni–B–Si_3N_4 composite coating).

The comparison of E_{corr} and i_{corr} values of ED Ni–B and Ni–B–Si_3N_4 composite coatings reveals that the extent of shift in E_{corr} towards the noble direction and decrease in i_{corr} value with the incorporation of Si_3N_4 particles in the ED Ni–B matrix is not appreciable and this trend is similar in both as-plated and heat-treated conditions. It has been established that high values of R_{ct} and low values of C_{dl} imply a better corrosion protective ability of coatings [29]. The C_{dl} value is related to the porosity of the coating [30]. The R_{ct} and C_{dl} values also did not show an appreciable change with the incorporation of Si_3N_4 particles in the ED Ni–B matrix, both in as-plated and heat-treated conditions. The occurrence of the second phase angle maximum suggests penetration of the electrolyte via the pores/micro-pores in these coating to create another interface, namely, the electrolyte/substrate. Hence, it is evident that incorporation of Si_3N_4 particles in the ED Ni–B

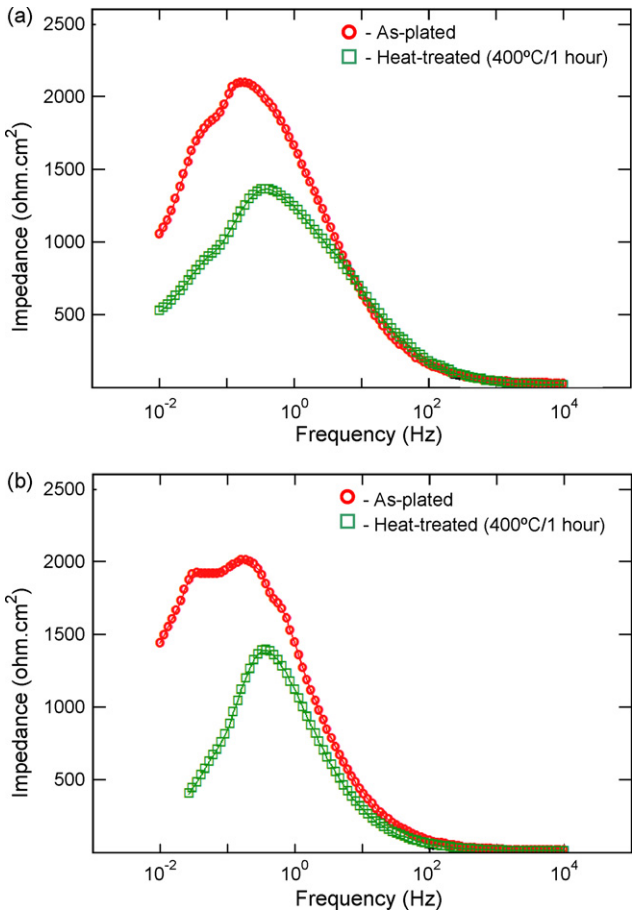

Fig. 6. Bode impedance plots of ED Ni–B and Ni–B–Si_3N_4 composite coatings in 3.5% NaCl in their as-plated and heat-treated (400 °C for h) at their respective open circuit potentials: (a) ED Ni–B; and (b) ED Ni–B–Si_3N_4.

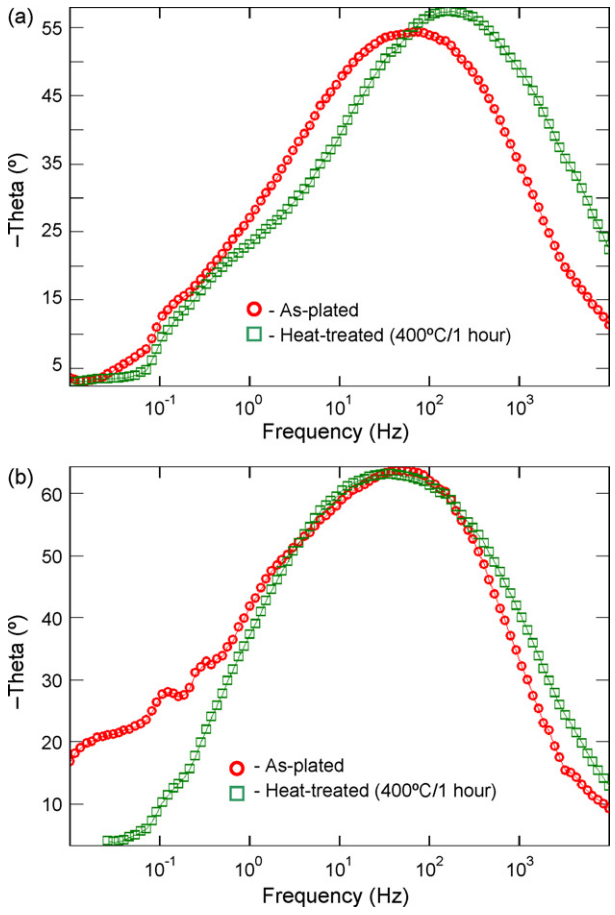

Fig. 7. Bode phase angle plots of ED Ni–B and Ni–B–Si_3N_4 composite coatings in 3.5% NaCl in their as-plated and heat-treated (400 °C for h) at their respective open circuit potentials: (a) ED Ni–B; and (b) ED Ni–B–Si_3N_4.

matrix enables only a marginal improvement in corrosion resistance.

Several factors, which include, coating thickness, porosity, composition of the coating, grain size, structure, surface features and heterogeneity of the coating, could influence the corrosion resistance of electro- and electroless plated deposits. In the present study, the coating thickness of both ED Ni–B and Ni–B–Si_3N_4 composite coatings used for evaluating the corrosion resistance is 20 ± 1 μm and they are uniform. Hence, contribution from thickness and uniformity is expected to be minimal. With the incorporation of Si_3N_4 particles in the ED Ni–B matrix, the chemical composition of coating changes from 97 wt.% Ni and 3 wt.% B to 89.6 wt.% Ni; 2.4 wt.% B and 8 wt.% Si_3N_4. XRD measurements reveal that incorporation of Si_3N_4 particles in the ED Ni–B matrix causes a change in crystal orientation. The grain size of as-plated ED Ni–B and Ni–B–Si_3N_4 composite coatings are 10–13 and 6–8 nm, respectively. Scanning electron micrographs of the ED Ni–B–Si_3N_4 composite coating reveal uniform distribution of the Si_3N_4 particles in the ED Ni–B matrix and the cracks in the coating are considerably reduced (Fig. 1). Heat-treatment (400 °C for 1 h) induces crystallinity of the ED Ni–B and ED Ni–B–Si_3N_4 composite coating, leading to the formation of crystalline Ni and Ni_3B phases and increases their grain size to 17–20 and 12–14 nm, respectively. The increase in grain boundaries following heat-treatment becomes the active sites for corrosion attack and causes a decrease in corrosion resistance.

The improvement or impairment of corrosion resistance of ED and EL composite coatings depends on the chemical stability of the particle, effective metallic area prone to corrosion, structural state or microstructural feature of the coating, porosity or defect size of the coating, ability to prevent diffusion of chloride ions along the interface between the metal and the particle, the ability of the particle to prevent the corrosive pits from growing up, etc. The Si_3N_4 particles are chemically stable in 3.5% NaCl. The incorporation of Si_3N_4 particles in the ED Ni–B matrix would decrease the effective metallic area prone to corrosion. The structural and morphological features (Figs. 1 and 2) indicate a change in microstructure and reduction in defects such as cracks and voids with the incorporation of Si_3N_4 particles in the ED Ni–B matrix. However, only a marginal improvement in the corrosion resistance of ED Ni–B–Si_3N_4 composite coatings compared to its plain counterpart is observed in this study. This could be due to the fact that unlike the nanosized particles, the micron size Si_3N_4 particles (mean diameter: 0.80 μm) used in this study is not capable of completely filling all the pores in the coating and allowed diffusion of chloride ions along the interface. The occurrence of a loop in the low frequency region in the Nyquist plot and the second phase angle maximum is the Bode phase angle plot confirms penetration of the chloride ions and creation of the electrolyte-substrate interface in both ED Ni–B and Ni–B–Si_3N_4 composite coatings. The marginal improvement in corrosion resistance observed for ED Ni–B–Si_3N_4 composite coatings compared to its plain counterpart could have resulted from the decrease in effective metallic area prone to corrosion.

4. Conclusions

The study aims to compare the corrosion resistance of ED Ni–B and Ni–B–Si_3N_4 composite coatings, both in as-plated and heat-

treated (400 °C for 1 h) conditions, in 3.5% NaCl. The characteristic properties, structural and morphological features were also determined to correlate the corrosion behaviour. The study leads to the following conclusions:

The incorporation of Si_3N_4 particles in the ED Ni–B matrix decreases the metallic lustre, increases the surface roughness and alters the chemical composition, causes a change in crystal orientation of the matrix and reduces the cracks in the coating.

The extent of shift in E_{corr} towards the noble direction, decrease in i_{corr}, increase in R_{ct} and decrease in C_{dl} values with the incorporation of Si_3N_4 particles in the ED Ni–B matrix is not appreciable, both in as-plated and heat-treated conditions.

The occurrence of second phase angle maximum confirms the penetration of the electrolyte via the pores/micro-pores in these coating.

The micron size Si_3N_4 particles (mean diameter: 0.80 μm) used in this study is not capable of completely filling all the pores in the coating and allowed diffusion of chloride ions along the interface.

The marginal improvement in corrosion resistance observed for ED Ni–B–Si_3N_4 composite coatings compared to its plain counterpart could have resulted from the decrease in effective metallic area prone to corrosion.

Acknowledgements

Financial support given to this work by the Council of Scientific and Industrial Research (CSIR), New Delhi, India was gratefully acknowledged. The authors are thankful to Prof. S.P. Mehrotra, Director, National Metallurgical Laboratory, Jamshedpur for his constant support and encouragement to carry out this research work.

References

[1] M. Musiani, Electrochim. Acta 45 (20) (2000) 3397.
[2] R.C. Agarwala, V. Agarwala, Sadhana 28 (3–4) (2003) 474.
[3] J.N. Balaraju, T.S.N. Sankara Narayanan, S.K. Seshadri, J. Appl. Electrochem. 33 (2003) 807.
[4] C.T.J. Low, R.G.A. Wills, F.C. Walsh, Surf. Coat. Technol. 201 (1–2) (2006) 371.
[5] M. Sarret, C. Müller, A. Amell, Surf. Coat. Technol. 201 (2006) 389.
[6] J.N. Balaraju, Electroless nickel composite coatings: Preparation and surface characterization, Ph.D. Thesis, Indian Institute of Technology-Madras, Chennai, 2000.
[7] C.S. Ramesh, S.K. Seshadri, Wear 255 (2003) 893.
[8] Y. Wang, S.C. Tung, Wear 225–229 (1999) 1100.
[9] Y. Xia, S. Sasaki, T. Murakami, M. Nakano, L. Shi, H. Wang, Wear 262 (2007) 765.
[10] L. Shi, C.F. Sun, F. Zhou, W.M. Liu, Mater. Sci. Eng. A. 397 (2005) 190.
[11] C.M. Das, P.K. Limaye, A.K. Grover, A.K. Suri, J. Alloys Compd. 436 (1–2) (2007) 328.
[12] J.N. Balaraju, T.S.N. Sankara Narayanan, S.K. Seshadri, Mater. Res. Bull. 41 (4) (2006) 847.
[13] J.N. Balaraju, K.S. Rajam, Int. J. Electrochem. Sci. 2 (2007) 747.
[14] J.N. Balaraju, K.S. Rajam, J. Alloys Compd. 459 (1–2) (2008) 311.
[15] L. Du, B. Xu, S. Dong, H. Yang, W. Tu, Wear 257 (2004) 1058.
[16] H. Xinmin, D. Zonggang, Plat. Surf. Finish. 80 (2) (1993) 62.
[17] K. Krishnaveni, T.S.N. Sankara Narayanan, S.K. Seshadri, Mater. Chem. Phys. 99 (2006) 300.
[18] T.S.N. Sankara Narayanan, S.K. Seshadri, J. Alloys Compd. 165 (2004) 197.
[19] K. Krishnaveni, T.S.N. Sankara Narayanan, S.K. Seshadri, Surf. Coat. Technol. 190 (2005) 115.
[20] K. Krishnaveni, T.S.N. Sankara Narayanan, S.K. Seshadri, J. Alloys Compd. 466 (1–2) (2008) 412.
[21] C. Muller, M. Sarret, M. Benballa, Surf. Coat. Technol. 162 (2002) 49.
[22] J. Novakovic, P. Vassiliou, Kl. Samara, Th. Argyropoulos, Surf. Coat. Technol. 201 (2006) 895.
[23] B. Bozzini, C. Martini, P.L. Cavallotti, E. Lanzoni, Wear 225–229 (1999) 806.
[24] A.G. McCormack, M.J. Pomeroy, V.J. Cunnane, J. Electrochem. Soc. 150 (5) (2003) C356.
[25] G. C^ar^ac, L. Benea, C. Iticescu, T. Lampke, S. Steinh¨auser, B. Wielage, Surf. Eng. 20 (5) (2004) 353.
[26] N.S. Qu, D. Zhu, K.C. Chan, Scripta Mater. 54 (2006) 1421.
[27] A. Contreras, C. Leon, O. Jimenez, E. Sosa, R. Perez, Appl. Surf. Sci. 253 (2) (2006) 592.
[28] F. Mansfeld, M. Kending, S. Tsai, Corrosion 38 (1982) 478.
[29] E.T. van Der Kouwe, Electrochim. Acta 38 (14) (1993) 2093.
[30] F.B. Growcock, R.J. Jasinski, J. Electrochem. Soc. 136 (8) (1989) 2310.